Supplementals

Heterologous expression of PtAAS1 reveals the metabolic potential of the common plant metabolite phenylacetaldehyde for auxin synthesis in planta

Jan Günther 1,3,*, Rayko Halitschke 2, Jonathan Gershenzon 1 and Meike Burow 3

1Max Planck Institute for Chemical Ecology, Department for Biochemistry, Hans-Knöll-Strasse 8, D-07745 Jena, Germany
2Max Planck Institute for Chemical Ecology, Department for Molecular Ecology, Hans-Knöll-Strasse 8, D-07745 Jena, Germany
3Department of Plant and Environmental Sciences, University of Copenhagen, Thorvaldsensvej 40, 1871 Frederiksberg C, Denmark

*Corresponding author
Jan Günther jg@plen.ku.dk

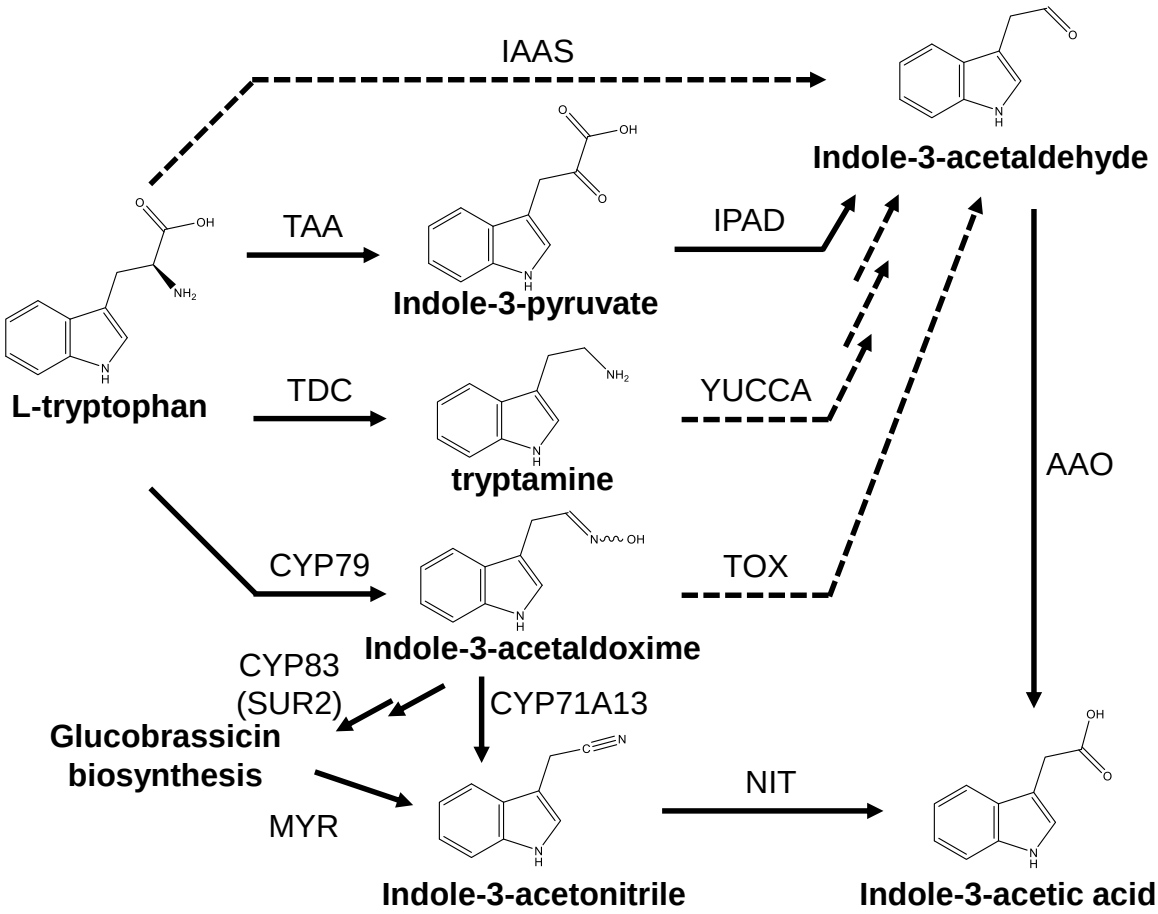

Supplemental Figure 1: Proposed, simplified pathways for the biosynthesis of indole-3-acetic acid in plants.

TAA, tryptophan aminotransferase; TDC, tryptophan decarboxylase; CYP79, cytochrome P450 family 79 enzyme; IAAS, indole-3-acetaldehyde synthase; IPA-DC, Indole-3-pyruvic acid decarboxylase; TOX, transoximase; AAO, aromatic aldehyde synthase; YUCCA, flavin monooxygenase-like enzyme; MYR, myrosinase; CYP83, cytochrome P450 family 83 enzyme; IPAD, indole-3-pyruvic acid decarboxylase. Dashed arrows, enzymes not characterized in plants; solid arrows, enzymes characterized in plants.

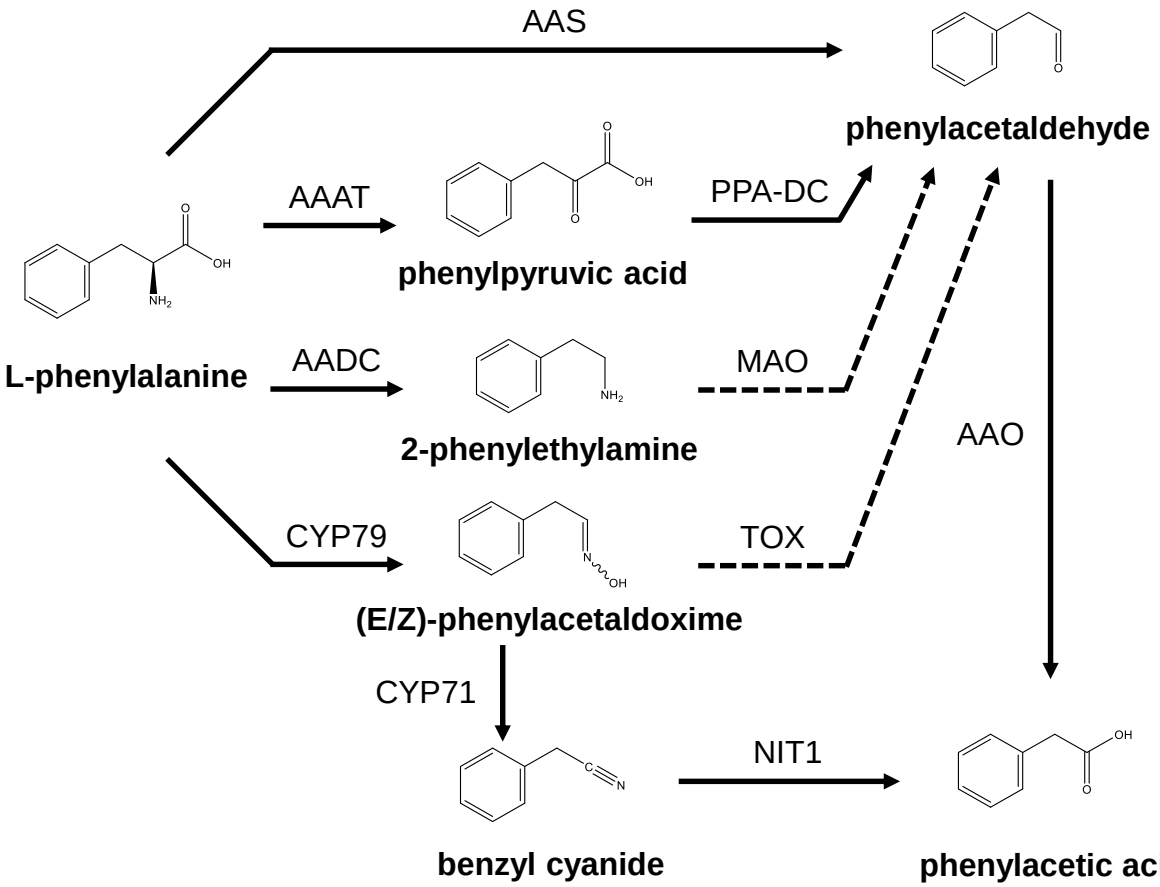

Supplemental Figure 2: Proposed pathways for the biosynthesis of phenylacetic acid in plants.

AAAT, aromatic amino acid transaminase; AADC, aromatic amino acid decarboxylase; CYP79, cytochrome P450 family 79 enzyme; PAAS, phenylacetaldehyde synthase; PPA-DC, phenylpyruvic acid decarboxylase; MAO, monoamine oxidase; TOX, transoximase; PAR, phenylacetaldehyde reductase; UGT, UDP-glucosyl transferase; β-Glu, β-glucosidase. Dashed line, enzymes not characterized in plants; solid line, enzymes characterized in plants.

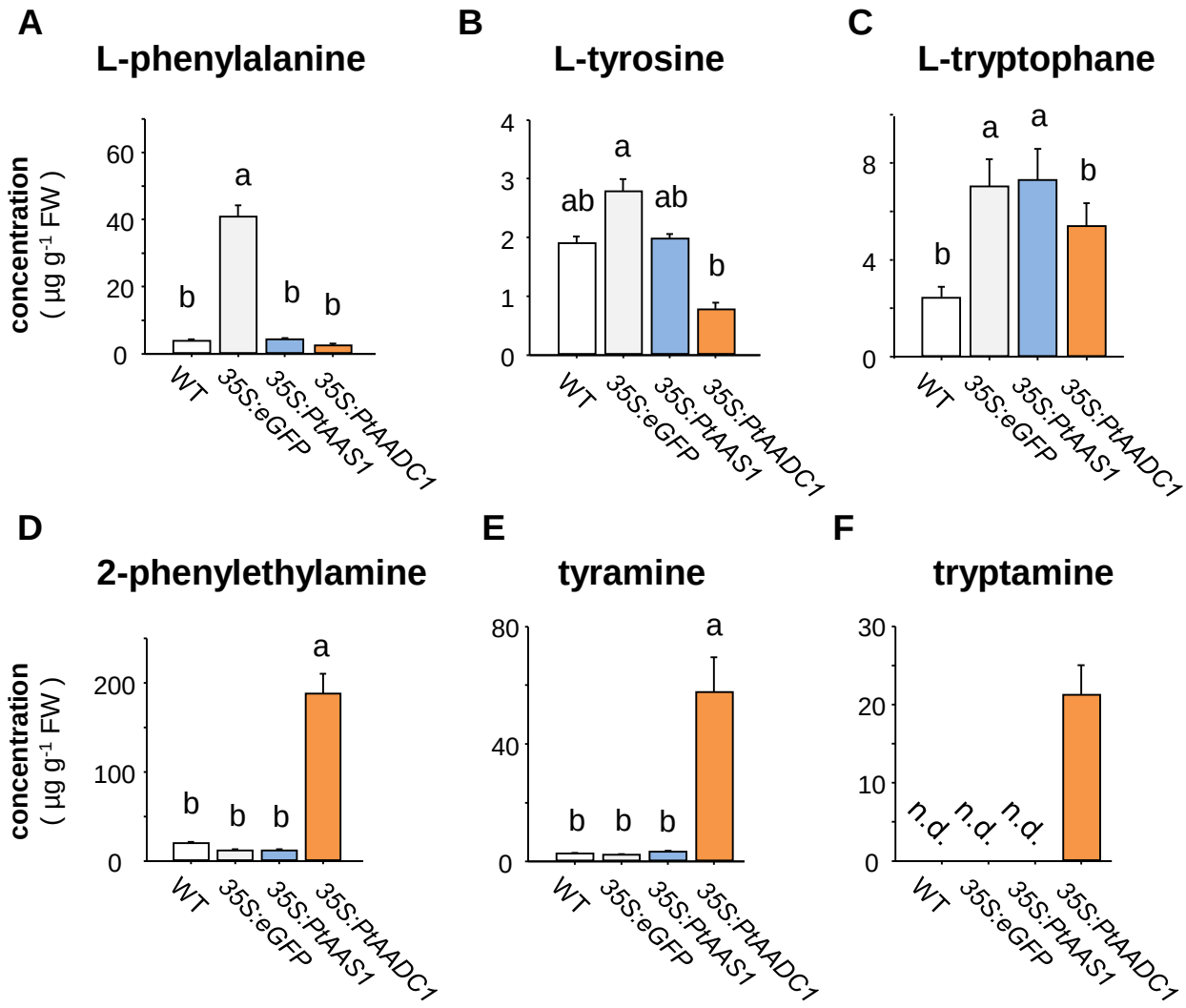

Supplemental Figure 3: Expression of *PtAADC1* results in decreased aromatic amino acid substrate pools (A-C) and accumulation of aromatic amine products (D-F) in *N. benthamiana* leaves.

The expression of poplar *PtAADC1* leads to the depletion of the aromatic amino acid substrates L-phenylalanine (A), L-tyrosine (B), and L-tryptophane (C) in expressing leaves. Accordingly, the corresponding enzymatic reaction products phenylethylamine (D), tyramine (E), and tryptamine (F) accumulate in *N. benthamiana* leaves, respectively. Different letters above each bar indicate statistically significant differences in Kruskal-Wallis One Way ANOVA and are based on the following Tukey test. Phe ($H = 16.58$, $P \leq 0.001$); Tyr ($F = 32.883$, $P \leq 0.001$); Trp ($F = 73.043$, $P \leq 0.001$); PEA ($H = 19.167$, $P \leq 0.001$); TyrA ($H = 17.34$, $P \leq 0.001$). Means + SE are shown ($n = 6$). FW, fresh weight. n.d., not detected.

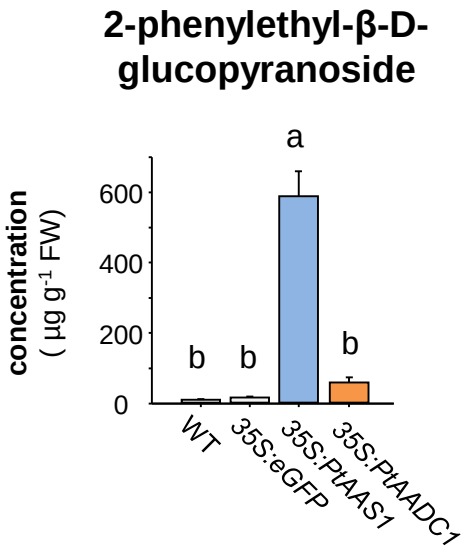

Supplemental Figure 4: Expression of *PtAADC1* and *PtAAS1* results in the increased accumulation of 2-phenylethyl-β-D-glucopyranoside in *N. benthamiana* leaves. *N. benthamiana* plants expressing *eGFP*, *PtAAS1, PtAADC1* and wild type plants were grown for 5 days post inoculation as described (Günther et al., 2019). The accumulation of 2-PEG in *N. benthamiana* leaves was analyzed via LC-MS/MS. Different letters above each bar indicate statistically significant differences in Kruskal-Wallis One Way ANOVA and Tukey test. 2-PEG ($H = 20.24$, $P \leq 0.001$). Means + SE are shown ($n = 6$). FW, fresh weight.

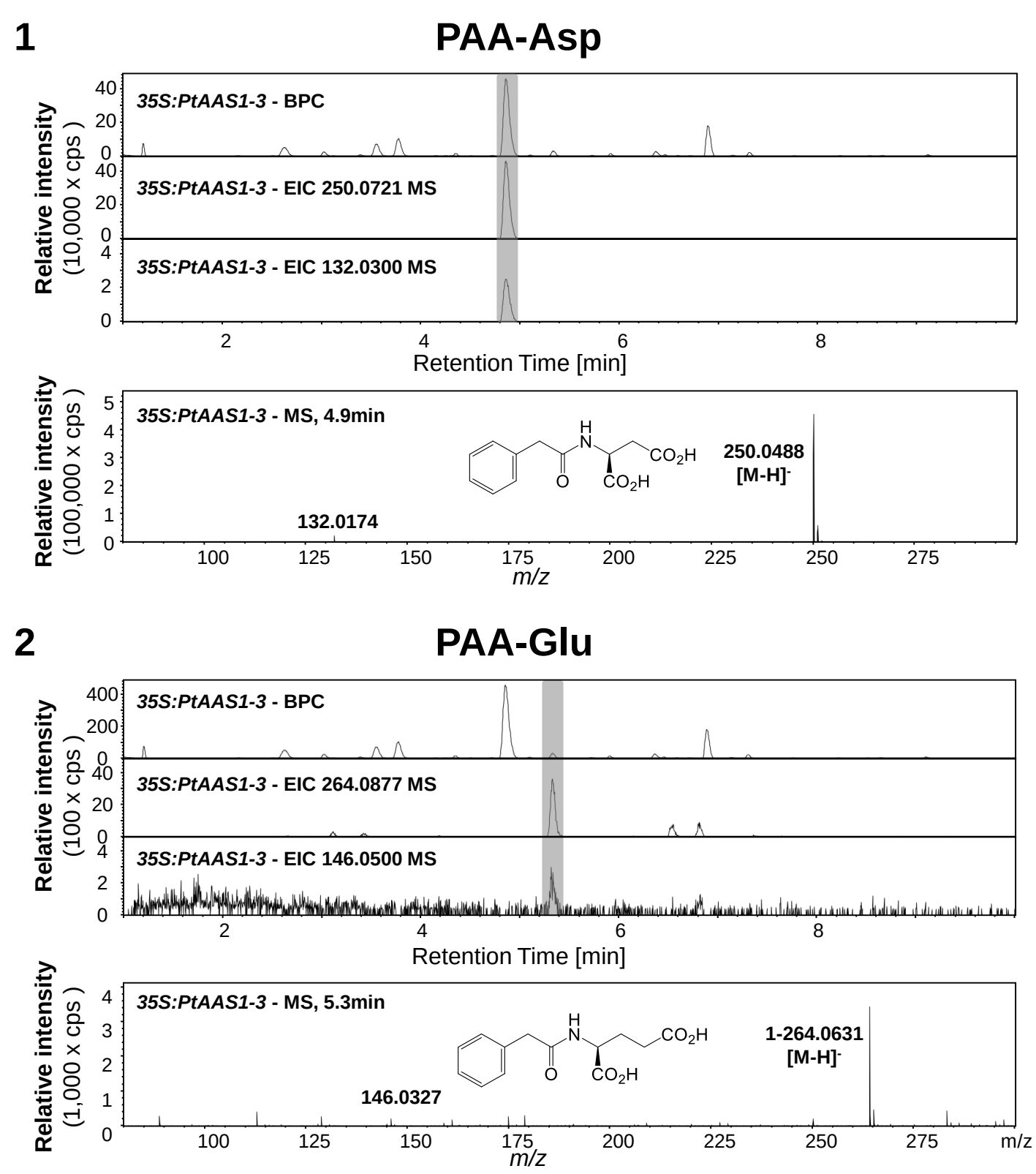

Supplemental Figure 5: LC-qToF-MS analysis of PAA conjugates in negative ionization mode.

The conjugates PAA-Asp (1) and PAA-Glu (2) could be identified from methanol extracts of leaves of *PtAAS1*-expressing *N. benthamiana*. Base peak chromatograms and extracted ion chormatograms are shown for the characteristic mother ion as well as one characteristic fragment (grey). Mass spectra of the in source fragmentation patterns for previously identified compounds PAA-Asp (1) and PAA-Glu (2) are shown. A representative sample of the total pool of replicates (n=6) was selected for visualization.

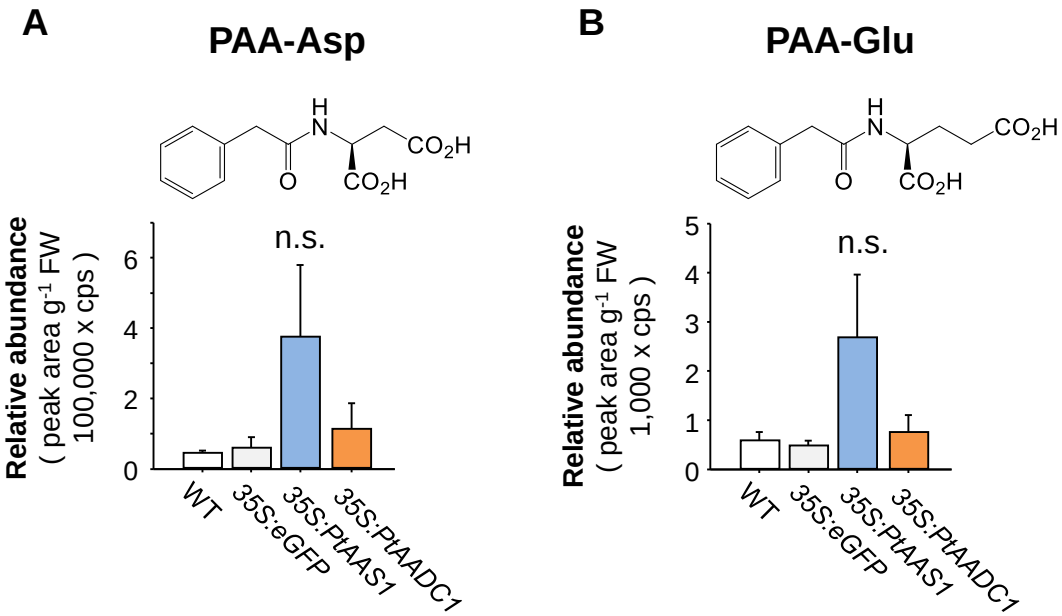

Supplemental Figure 6: Expression of *PtAAS1* results in unaltered abundance of auxin conjugates PAA-Asp (A) and PAA-Glu (B) in *N. benthamiana* roots. The identified conjugates were analyzed for a characteristic fragmentation via LC-MS/MS. Means + SE are shown (n = 6). FW, fresh weight. n.s., not significant

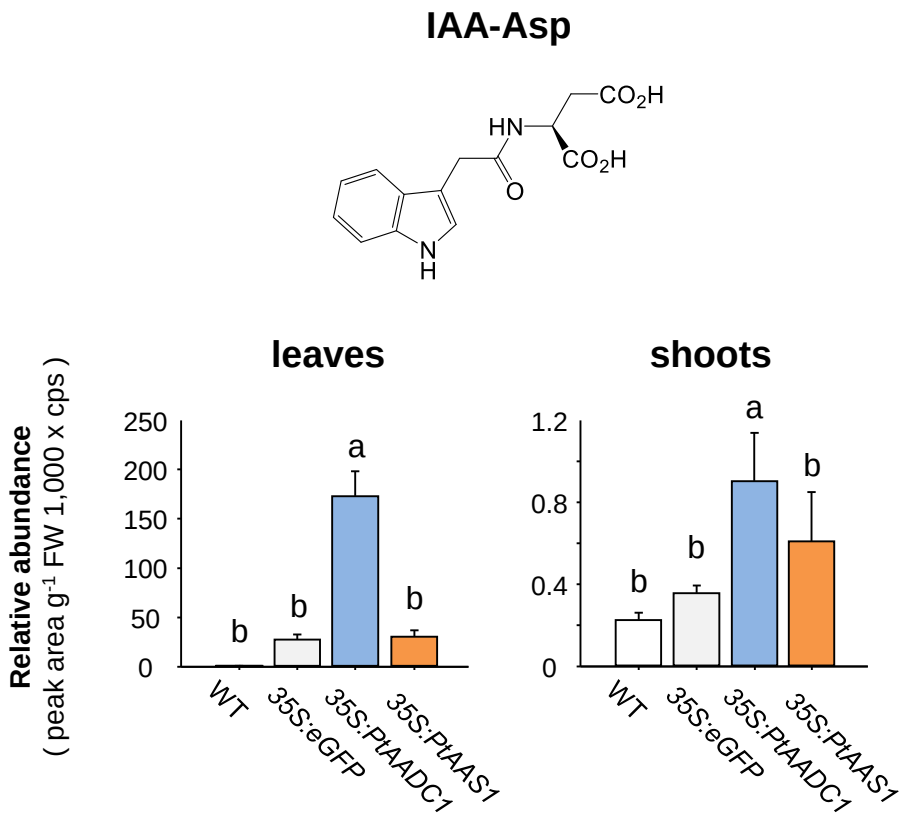

Supplemental Figure 7: Expression of *PtAAS1* results in increased levels of the auxin conjugate IAA-Asp in *N. benthamiana* shoots and leaves. The identified conjugates were analyzed for a characteristic fragmentation via LC-MS/MS. Relative quantification of the identified conjugates IAA-Asp. Different letters above each box indicate statistically significant differences in Kruskal-Wallis One Way ANOVA and are based on the following Tukey test. $IAA\text{-}Asp_{Shoots}$ ($H = 15.173$, $P = 0.002$); $IAA\text{-}Asp_{Leaves}$ ($H = 19.547$, $P \leq 0.001$). Means + SE are shown ($n = 6$) FW, fresh weight.

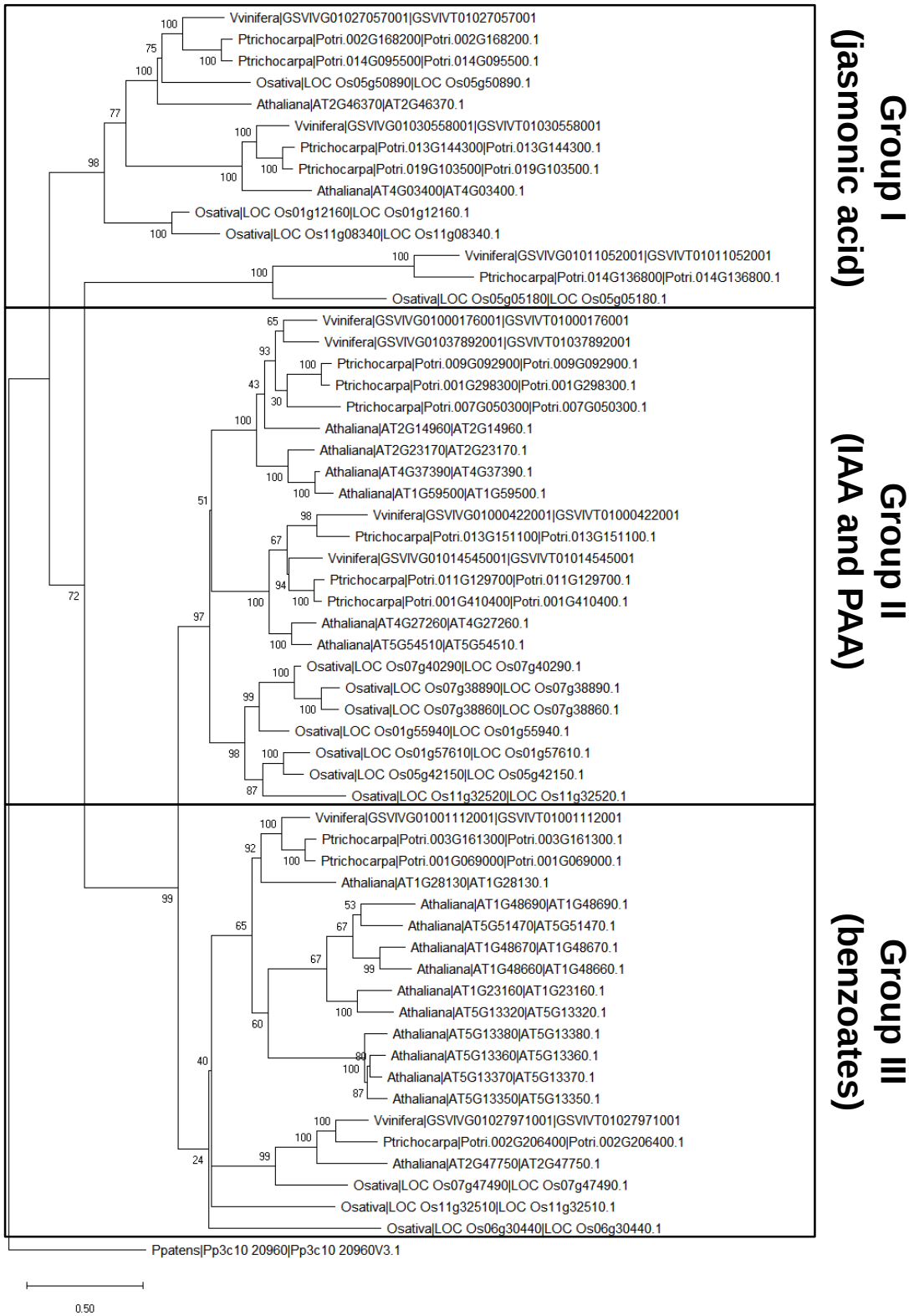

Supplemental Figure 8: Phylogenetic reconstruction of identified and characterized GH3 auxin-amido synthetases coding sequences. Putative GH3 auxin-amido synthetase sequences from *Populus trichocarpa* and recently identified and characterized GH3 auxin-amido synthetases from *Oryza sativa*, *Arabidopsis thaliana*, and *Vitis vinifera*. Each group I - III is highlighted in rectangles and labeled with characteristic substrates. A putative GH3 from *Physcomitrella patens* served as outgroup. The tree was inferred by using the maximum likelihood method and n = 1,000 replicates for bootstrapping. Bootstrap values are shown next to each node. Relative branch lengths measure the number of substitutions per site.

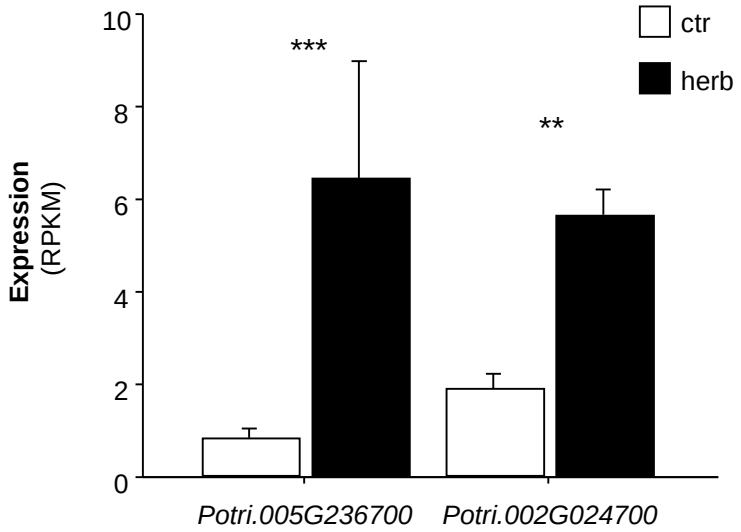

Supplemental Figure 9: Transcript accumulation of *Aux/IAA* genes in *L. dispar*-damaged and undamaged *Populus trichocarpa* leaves. Gene expression in herbivore-damaged (herb) and undamaged (ctr) leaves was analyzed by Illumina sequencing and mapping the reads to the transcripts of the *P. trichocarpa* genome version v3.0. Expression was normalized to RPKM. Significant differences in EDGE tests are visualized by asterisks. Means + SE are shown (n = 4). *Potri.005G236700* (P = 4.06063E-05, weighted difference (WD) = 8.81922E-06); *Potri.002G024700* (P = 0.005250486, WD = 6.0016E-06).

Table S3

HPLC conditions (gradients) used for separation and analysis of plant metabolites. See also Supplemental Table 2 for MS/MS parameters.

	Time (min)	**Flow** (µl/min)	**Water 0.5% FA** (%)	**Acetonitrile** (%)
Gradient A (auxins sched MRM)	0	1100	95	5
	0.5	1100	95	5
	6.0	1100	62.6	37.4
	6.02	1100	0	100
	7.5	1100	0	100
	7.6	1100	95	5
Gradient B (auxin-conjugates)	0	1100	95	5
	0.5	1100	95	5
	6	1100	62.6	37.4
	6.02	1100	20	80
	7.5	1100	0	100
	9.5	1100	0	100
	9.52	1100	95	5
Gradient C (amines and amino acids)	0	1100	97	3
	1	1100	97	3
	2.7	1100	0	100
	3	1100	0	100
	3.1	1100	97	3
	6	1100	97	3

Table S4

MS/MS parameters used for LC-MS/MS analysis. The details of the HPLC gradients indicated in the right column are given in Supplemental Table 2.

compound	Q1	Q3	Scan time (ms)	DP	EP	CE	CXP	mode	HPLC gradient
phenylacetic acid[1]	134.854	91	1000	-30	-8.5	-10	-10	neg	B
PAA-Asp[2]	250.1	132.1	20	-30	-8.5	-15	-10	neg	A
PAA-Glu[2]	264.173	146.1	20	-30	-8.5	-15	-10	neg	A
IAA-Asp[3]	289	132	20	-55	-9	-24	-10	neg	A
4-OH-PAA[1]	151.05	107.0	1000	-30	-8.5	-10	-10	neg	B
2-PEG[4]	329.015	45	20	-30	-5.5	-24	0	neg	A
IAA[1]	176	130	10	40	10	19	16	pos	C
Phe[4]	166.2	120.2	10	30	6	17	4	pos	C
Tyr[4]	182.1	136.2	10	30	7	17	4	pos	C
Trp[4]	205.2	188.1	10	30	4.5	13	6	pos	C
PEA[5]	122.01	105	10	30	4	15	4	pos	C
TyrA[5]	138.01	121	10	30	4	15	4	pos	C
TrpA[5]	181.2	144.2	10	30	8	17	4	pos	C

References:

1. **Günther J, Irmisch S, Lackus ND, Reichelt M, Gershenzon J, Köllner TG** (2018) The nitrilase PtNIT1 catabolizes herbivore-induced nitriles in Populus trichocarpa. BMC Plant Biol **18**: 1–12

2. **Sugawara S, Mashiguchi K, Tanaka K, Hishiyama S, Sakai T, Hanada K, Kinoshita-tsujimura K, Yu H, Dai X, Takebayashi Y, et al** (2015) Distinct Characteristics of Indole-3-Acetic Acid and Phenylacetic Acid , Two Common Auxins in Plants. **56**: 1641–1654

3. **Westfall CS, Sherp AM, Zubieta C, Alvarez S, Schraft E, Marcellin R, Ramirez L, Jez JM** (2016) *Arabidopsis thaliana* GH3.5 acyl acid amido synthetase mediates metabolic crosstalk in auxin and salicylic acid homeostasis. Proc Natl Acad Sci **113**: 13917–13922

4. **Irmisch S, Clavijo McCormick A, Boeckler GA, Schmidt A, Reichelt M, Schneider B, Block K, Schnitzler J-P, Gershenzon J, Unsicker SB, et al** (2013) Two Herbivore-Induced Cytochrome P450 Enzymes CYP79D6 and CYP79D7 Catalyze the Formation of Volatile Aldoximes Involved in Poplar Defense. Plant Cell **25**: 4737–4754

5. **Günther J, Lackus ND, Schmidt A, Huber M, Stödler H-J, Reichelt M, Gershenzon J, Köllner TG** (2019) Separate pathways contribute to the herbivore-induced formation of 2-phenylethanol in poplar. Plant Physiol **180**: pp.00059.2019

Table S5

Compounds used as standards for LC-MS/MS quantification.

Compound	CAS	Supplier
L-phenylalanine	63-91-2	Duchefa
L-tyrosine	60-18-4	Duchefa
L-tryptophan	73-22-3	SigmaAldrich
2-phenylethylamine	156-28-5	Santa Cruz
tyramine	60-19-5	Roth
tryptamine	61-54-1	AppliChem
2-phenylethyl-β-D-glucopyranoside	18997-54-1	Toronto Research Chemicals
Indole-3-acetic acid	87-51-4	Duchefa
4-hydroxy phenylacetic acid	156-38-7	Acros
phenylacetic acid	103-82-2	Aldrich